




Turbulence-mediated facilitation of resource uptake in patchy stream macrophytes

Loreta Cornacchia ^{1,2,a*} Sofia Licci ³ Heidi Nepf,⁴ Andrew Folkard ⁵ Daphne van der Wal,^{1,6} Johan van de Koppel,^{1,2} Sara Puijalon,³ Tjeerd J. Bouma^{1,2}

¹NIOZ Royal Netherlands Institute for Sea Research, Department of Estuarine and Delta Systems, and Utrecht University, P.O. Box 140, 4400 AC Yerseke, The Netherlands

²Groningen Institute for Evolutionary Life Sciences, University of Groningen, Groningen, The Netherlands

³Univ Lyon, Université Claude Bernard Lyon 1, CNRS, ENTPE, UMR 5023 LEHNA, Villeurbanne, France

⁴Department of Civil and Environmental Engineering, Massachusetts Institute of Technology, Cambridge, Massachusetts

⁵Lancaster Environment Centre, Lancaster University, Lancaster, United Kingdom

⁶Faculty of Geo-Information Science and Earth Observation, University of Twente, Enschede, The Netherlands

Abstract

Many landscapes are characterized by a patchy, rather than homogeneous, distribution of vegetation. Often this patchiness is composed of single-species patches with contrasting traits, interacting with each other. To date, it is unknown whether patches of different species affect each other's uptake of resources by altering hydrodynamic conditions, and how this depends on their spatial patch configuration. Patches of two contrasting aquatic macrophyte species (i.e., dense canopy-forming *Callitriche* and sparse canopy-forming *Groenlandia*) were grown together in a racetrack flume and placed in different patch configurations. We measured ¹⁵NH₄⁺ uptake rates and hydrodynamic properties along the centerline and the lateral edge of both patches. When the species with a taller, denser canopy (*Callitriche*) was located upstream of the shorter, sparser species (*Groenlandia*), it generated turbulence in its wake that enhanced nutrient uptake for the sparser *Groenlandia*. At the same time, *Callitriche* benefited from being located at a leading edge where it was exposed to higher mean velocity, as its canopy was too dense for turbulence to penetrate from upstream. Consistent with this, we found that ammonium uptake rates depended on turbulence level for the sparse *Groenlandia* and on mean flow velocity for the dense *Callitriche*, but Total Kinetic Energy was the best descriptor of uptake rates for both species. By influencing turbulence, macrophyte species interact with each other through facilitation of resource uptake. Hence, heterogeneity due to multispecific spatial patchiness has crucial implications for both species interactions and aquatic ecosystem functions, such as nitrogen retention.

In many ecosystems, vegetation shapes entire landscapes by interacting with physical processes (Dietrich and Perron 2006; Corenblit et al. 2011). In coastal and fluvial aquatic ecosystems, vegetation modifies habitats through its effects on hydrodynamics and sedimentation (Leonard and Luther 1995; Madsen et al. 2001; Schulz et al. 2003; Bouma et al. 2007), hence acting as an ecosystem engineer (Jones et al. 1994). Many studies first considered interactions between hydrodynamics and homogeneous vegetation (Kouwen and Unny 1973; Nepf 1999; Nepf and Vivoni 2000; Järvelä 2005; Chen

et al. 2013) and later focused on isolated or pairs of patches (Sand-Jensen and Vindbæk Madsen 1992; Folkard 2005; Bouma et al. 2009; Vandenbruwaene et al. 2011; Chen et al. 2012; Zong and Nepf 2012). Generally, vegetation patches locally reduce flow velocities, while increasing them in some adjacent areas (Bouma et al. 2007; Chen et al. 2012; Schoelynck et al. 2012; Meire et al. 2014).

In aquatic ecosystems, the interaction between vegetation and hydrodynamics regulates important ecological processes such as nutrient delivery and uptake by plants, as nutrients can be taken up from the water column through plant shoots (Madsen and Cedergreen 2002; Bal et al. 2013). These processes are crucial for community primary productivity and ecosystem function (Thomas et al. 2000; Morris et al. 2008; Levi et al. 2015). Previous studies on uptake rates in relation to hydrodynamic conditions mainly focused on seagrasses, using flume experiments with dissolved ¹⁵N-labeled ammonium or nitrate

*Correspondence: loreta.cornacchia@univ-lyon1.fr

^aPresent address: UMR 5023 LEHNA, Université Lyon 1, CNRS, ENTPE, Villeurbanne, France

Additional Supporting Information may be found in the online version of this article.

(often the main inorganic nitrogen sources in natural conditions; Haynes and Goh 1978). These works identified the important effects of water velocity and flow alteration by seagrass canopies on resource uptake (Thomas et al. 2000; Cornelisen and Thomas 2006), and the dependence of uptake rates on the rate of mass transfer to the leaf surface under unidirectional flow (Cornelisen and Thomas 2004). Further, Morris et al. (2008) identified spatial patterns in ammonium uptake within seagrass patches, with higher uptake observed at the leading edge of the patch where the turbulent kinetic energy and velocity within the patch were highest. In a study of nutrient uptake by river macrophytes, Bal et al. (2013) found that ammonium uptake increased with flow velocity. Because the diffusive boundary layer decreases with increasing velocity, the uptake rate also increases with increasing velocity (Thomas et al. 2000; Cornelisen and Thomas 2004; Morris et al. 2008; Bal et al. 2013).

However, most of the previous studies dealt with monospecific canopies or focused on a single species at a time, creating a monospecific community, while in reality natural landscapes are a diverse community made up of multiple species. Different patches of single species are heterogeneously distributed, and this patchiness is a common characteristic of aquatic habitats (Sand-Jensen and Vindbæk Madsen 1992). A few examples are patchy seagrass meadows (Fonseca et al. 1983), and streams characterized by a “pseudobraided” distribution of plant stands between areas of faster flow (Dawson and Robinson 1984; Cotton et al. 2006; Wharton et al. 2006). This additional level of complexity has just started to be integrated in studies of hydrodynamic-vegetation interactions. For instance, Weitzman et al. (2015) focused on hydrodynamic implications of multispecific canopies but considered canopy heterogeneity in the vertical dimension. Adhitya et al. (2014) focused on hydrodynamics and spatial configurations of seagrass patches with different densities but did not test the consequences for resource uptake. Bal et al. (2013) focused on nutrient uptake rates within monospecific patches of two species next to each other, but they only tested a single spatial configuration and therefore did not investigate the effects of spatial patchiness. To date, it is still unknown how patches of different species interact with each other by altering hydrodynamics and uptake of resources and how this depends on their landscape configuration.

Multispecies effects could be important for hydrodynamics and nutrient uptake because the density, flexibility, and

canopy structure of different species affect hydrodynamics differently (Peralta et al. 2008; Bouma et al. 2013). As we cannot easily predict the flow alteration by heterogeneous species distributions, our understanding of the implications for species interactions and nutrient load reduction in aquatic ecosystems is limited. Generally, the hydrodynamic controls on uptake rate are expected to be dependent on the macroscale rate of delivery (mean flow velocity; e.g., Cornelisen and Thomas 2006) or on the microscale processes that determine the concentration gradient at the leaf boundary layer (turbulence; e.g., Morris et al. 2008). However, in a diverse community, there might be cases where a single hydrodynamic parameter is not sufficient to describe uptake rates for multiple species with different traits and effects on hydrodynamic conditions. For instance, turbulence can have a significantly smaller scale in very dense canopies, compared to sparser ones (Nepf 2012). Conversely, the mean flow speed can be relatively constant within sparse canopies, but turbulence might be locally variable. Therefore, understanding the interaction between multiple species in terms of nutrient uptake, mediated by their hydrodynamic effects, is essential to gain a more realistic understanding of species interactions and productivity in heterogeneous, multispecific communities.

In this study, we use streams colonized by aquatic macrophytes as a model system. We investigate how patches of two different species with contrasting morphological traits interact with each other by influencing hydrodynamics, and thereby ammonium uptake. Moreover, we test how this depends on their spatial configuration (patchiness). Here, we define multispecific patchiness as a community composed of patches of different species. Specifically, we study the interaction between two macrophyte species that co-occur under field conditions and have contrasting density and canopy structure: *Callitriche platycarpa* Kütz., 1842, forms very dense patches that exhibit increasing canopy height with increasing patch length (“dense” species); and *Groenlandia densa* (L.) Fourr. has a more open canopy, and its canopy height is constant along the patch length (“sparse” species). In the field, the dense patches of *Callitriche* are distributed quite regularly at a distance of about 8 m, and *Groenlandia* patches tend to aggregate around them (Cornacchia et al. 2018). Given the differences in shoot density and canopy architecture between the two species (Table 1), we hypothesize that the effects of the dense *Callitriche* patches on hydrodynamics may facilitate the

Table 1. Summary of patch characteristics (mean \pm SD [n]) of the two species at the incoming flow velocity of 0.24 m s^{-1} used in the flume experiments: Biomass (g DW m^{-2} ; measured), canopy height (h , m; measured), frontal area per water volume (a , m^{-1} ; calculated from Eq. 3), and frontal area per bed area (ah , dimensionless; calculated from Eq. 4).

| | Biomass (g [DW] m^{-2}) | Canopy height (h , m) | Frontal area per water volume (a , m^{-1}) | Frontal area per bed area (ah , dimensionless) |
|--------------------|---------------------------------------|-----------------------------|--|--|
| <i>Groenlandia</i> | 97 ± 28 (3) | 0.070 ± 0.010 (9) | 0.090 ± 0.007 (2) | 0.031 ± 0.003 (2) |
| <i>Callitriche</i> | 318 ± 67 (3) | 0.170 ± 0.080 (5) | 0.571 ± 0.101 (2) | 0.200 ± 0.035 (2) |

delivery and uptake of resources by the sparse *Groenlandia* patches. To test this hypothesis, patches of the two species were arranged in different configurations in a laboratory flume. To investigate the role of spatial configuration and reciprocal species effects on nutrient uptake, both the species upstream and the relative location of the species downstream were varied. We discuss the implications of multi-specific spatial patchiness on facilitation and aquatic ecosystem functions, such as nitrogen retention.

Materials and methods

Plant material

We tested the effect of macrophyte patch species and configuration on ammonium uptake rates using two submerged macrophytes species, *Callitriche platycarpa* and *Groenlandia densa*. Both species were collected in February 2015 from a wetland on the Ain River, France (5.2825°E, 45.9855 N). Plants were stored in plastic bags and transported to the laboratory in NIOZ Yerseke (The Netherlands) within 24 h from collection. Until installation in the flume, the two macrophyte species were stored in a green house, in tanks filled with freshwater that was continuously aerated, and exposed to natural light. The macrophytes were allowed to recover for 2 d in the green house before starting the experiments. In order to be

used for the experimental setup, individual plants were transplanted in stainless steel trays (30 × 29.5 × 5 cm). The trays were filled with a bottom layer of river sand (4.5 cm) and a top layer (0.5 cm) of fine gravel (0.2 cm grain size). A false bottom in the flume allowed the trays to be inserted with the soil surface at the same level as the flume bed. Based on the naturally occurring densities of the two species in the field, we constructed patches of 97 ± 28 g DW m⁻² (mean ± SD) for *Groenlandia* (“sparse” species) and 318 ± 67 g DW m⁻² for *Callitriche* (“dense” species) (Fig. 1; Table 1). The biomass of the constructed patches was estimated by collecting all plant material within randomly selected 0.1 × 0.1 m quadrants ($n = 3$). The mean patch biomass for *Callitriche* is close to the range of 208–256 g DW m⁻² reported in Sand-Jensen and Vindbæk Madsen (1992). The mean patch biomass for *Groenlandia* corresponded to ca. 500 shoots m⁻², which represents a relatively low shoot density in natural plant beds (Sheldon and Boylen 1977). We used a different patch length for each species to resemble the typical lengths observed in the field, that is, 2.7 and 1.2 m on average for *Groenlandia* and *Callitriche*, respectively. These values are representative of average patch sizes observed in field conditions (2.5 ± 1.7 m for *Groenlandia*, $n = 20$; 1.4 ± 0.8 m for *Callitriche*, $n = 20$; Supporting Information Fig. S1). We used a total of nine trays for *Groenlandia*, for a total patch coverage of 2.7×0.3 m. For

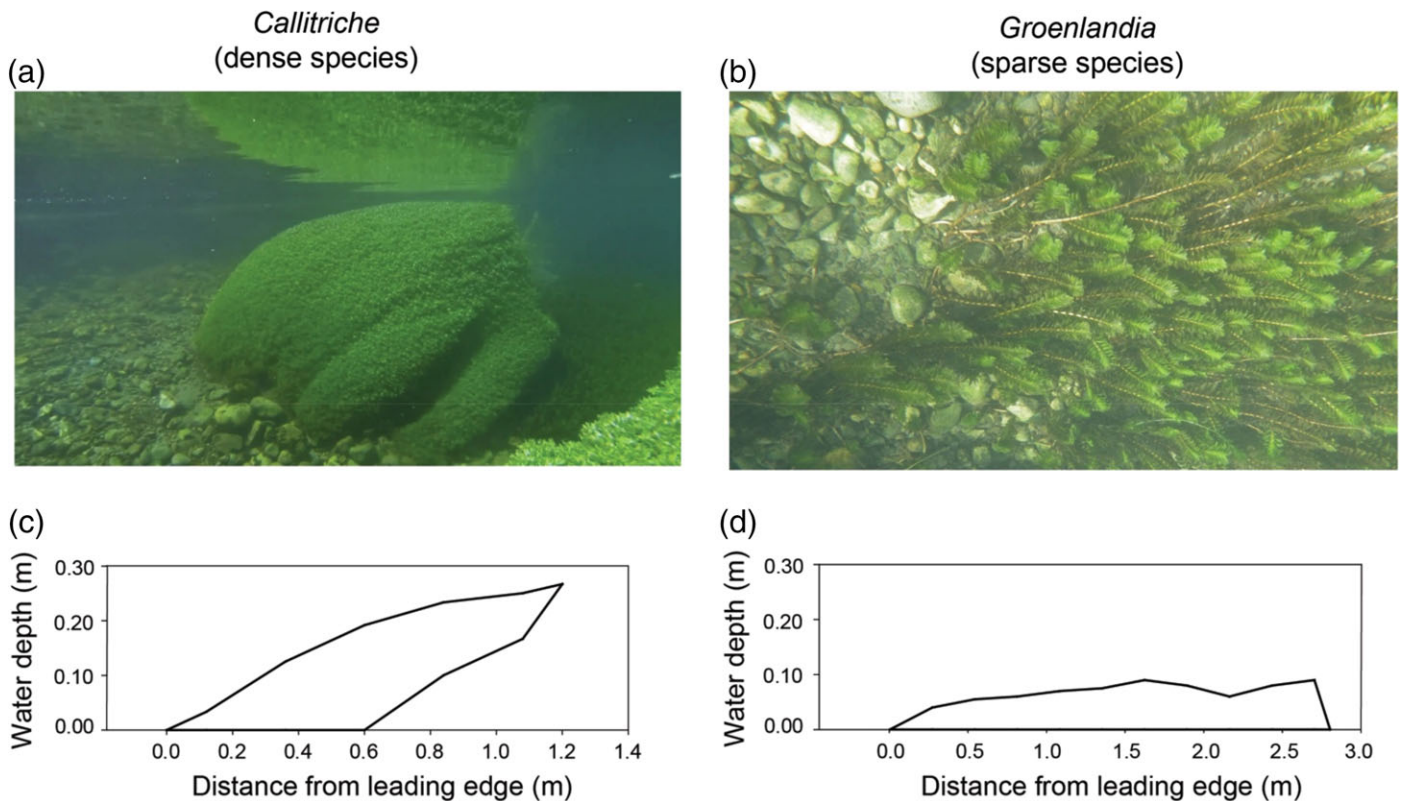


Fig. 1. Natural patches of (A) *Callitriche* and (B) *Groenlandia* in the field. (C, D) lateral view of the two patches, with the black outline indicating canopy height at increasing distance from the patch leading edge.

Callitriche, plants were rooted in two trays ($0.6 \times 0.3 \times 0.05$ m). When *Callitriche* was placed upstream, three trays (filled with the same soil as the plant trays) were placed between the two patches, to account for the presence of the typical overhanging canopy for this species. That is, when the flume was running, a total coverage of 1.20×0.3 m² was observed due to shoots bending; this region was considered as part of the *Callitriche* patch (see Fig. 2). A distance of one tray (0.3 m) between the two patches was used for the configurations in which *Groenlandia* was in the upstream position. The flume section next to each patch was left open (without

plants, but filled with the same soil substrate used in the plant trays) in all configurations. Thus, the patches occupied one half of the flume, rather than extending across the width of the flume. As patches in the field do not span the whole channel, this configuration is representative of the typical distribution of vegetation patches in streams, with an empty (unvegetated) zone next to the patch into which water flow is deflected and accelerated around the patch (Fonseca et al. 1983; Gambi et al. 1990; Bouma et al. 2007; Follett and Nepf 2012). The canopies of both species were fully submerged during the experiments. The relative depth of submergence (H/h , ratio of water

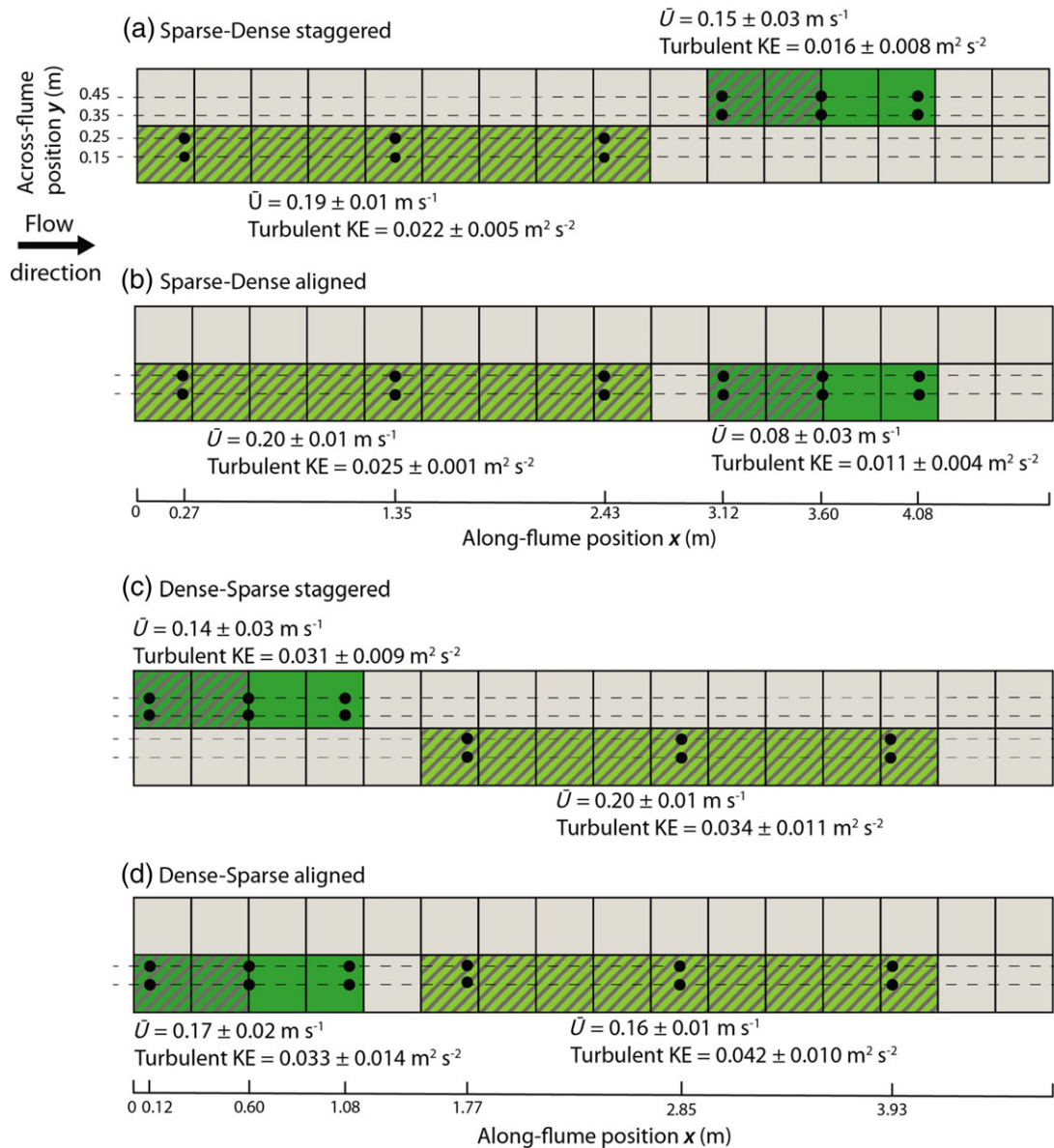


Fig. 2. Schematic diagram of the four spatial configurations of aquatic macrophytes in the test section of the flume: (a) Sparse-Dense staggered, (b) Sparse-Dense aligned, (c) Dense-Sparse staggered, and (d) Dense-Sparse aligned. Light green indicates patches of *Groenlandia* (sparse canopy), and dark green indicates patches of *Callitriche* (dense canopy). Diagonal lines indicate the boxes in which plants were rooted. Black circles are locations of plant specimens removed after the incubations experiments for assessment of NH_4^+ uptake rates, and of acoustic ADV profile measurements. Numbers indicate mean (\pm SE) water velocity \bar{U} (m s^{-1}) and turbulent KE ($\text{m}^2 \text{s}^{-2}$) within each species patch.

depth to maximum canopy height; Nepf 2012) was relatively constant along the *Groenlandia* patch due to its uniform height. Values of H/h ranged between 8.75 and 4.3, corresponding to shallow submerged ($H/h < 5$). Instead, canopy height along the *Callitriche* patch varied from $H/h = 17.5$ at the leading edge (i.e., deeply submerged, $H/h > 10$) to 3.0 in the middle of the patch (indicating shallow submergence, $H/h < 5$), and even 1.30 at the downstream end of the patch, which is very close to emergent conditions ($H/h = 1$).

Flume setup and experimental configurations

All experiments were performed within a unidirectional racetrack flume using a water depth of 0.35 m and with a cross-sectionally averaged velocity of $0.24 \pm 0.03 \text{ m s}^{-1}$. This is a moderate flow velocity, representative of the summer flow conditions in streams typically colonized by *Callitriche* and *Groenlandia* ($0.21 \pm 0.01 \text{ m s}^{-1}$, based on our field measurements in 2014 and 2015; Cornacchia et al. 2018). For a more detailed description of the flume, see Bouma et al. (2005). To test for the effects of patch spatial configuration on ammonium uptake rates, the two patches were arranged one downstream of the other, either on the same side of the flume (“aligned” configurations) or on opposite sides (“staggered” configurations) (Fig. 2). These different spatial configurations are both commonly observed in natural streams, where patches grow downstream of other patches, or in a staggered arrangement (L. Cornacchia pers. obs.). Moreover, patches of different species in the field can be found co-occurring at very short distances from each other, at the scale of 0.5 m (Cornacchia et al. 2018). To test for interactions between the two species, in terms of reciprocal effects on ammonium uptake rates, we also switched the species located upstream for each of these configurations (“sparse–dense” [S-D] or “dense–sparse” [D-S] configurations).

Measuring spatial patterns in $^{15}\text{N-NH}_4^+$ uptake rates and canopy hydrodynamics

To determine spatial patterns of ammonium uptake rates by the macrophyte species, we measured uptake rates at selected locations within the patches (Fig. 2). Nutrient uptake rates were determined inside the two patches at 10%, 50%, and 90% of the patch length (0.27, 1.45, and 2.43 m from the leading edge in *Groenlandia*; 0.12, 0.6, and 1 m from the leading edge in *Callitriche*) and, for each location along the patch length, at 0.15 and 0.25 m of the patch width. For each incubation experiment, macrophyte individuals were randomly selected from the tanks where they were kept with freshwater and were transplanted into plastic pots (five shoots per pot). Before transplantation in the flume, roots were removed from the plants at the selected test locations, to prevent ammonium uptake by that means from the labeled water that inevitably penetrated into the sand (following Bal et al. 2013). As the sediment was not changed in between treatments (as that would have meant destroying and recreating the patches), this

avoided an effect of treatment order on uptake rates. While some nutrients are obtained through roots in field conditions, the nutrient demands of many macrophyte species can be satisfied by shoot nutrient uptake alone (Madsen and Cedergreen 2002). Although root removal may have potentially affected the plant response to the flow, it was unlikely to affect their ability to resist the flow during a short-term experiment (6 h). Each plastic pot was then placed in one of the patch locations described above and inserted in the trays so that their upper part was in line with the sediment level to avoid scouring effects. The pots were replaced after each incubation experiment, and new plants were transplanted. The renewal of plants between each run allowed us to avoid an effect of treatment order on uptake rates due to plants being exposed to the labeled water for a longer time. Moreover, it provided natural variability in plant structure, while maintaining a constant patch structure by keeping the trays forming the plant patches in the same positions between runs. The treatments were run in the order shown in Fig. 1.

In the incubation experiments, $^{15}\text{N-NH}_4^+$ was added to the water creating a 20–30 $\mu\text{mol NH}_4^+ \text{ L}^{-1}$ solution, with 30% of the N as ^{15}N abundance, following Bal et al. (2013). This range of values is representative of nutrient concentrations found in natural ecosystems: in summer 2015, average ammonium levels recorded in the studied region were $24.5 \pm 28.54 \mu\text{mol NH}_4^+ \text{ L}^{-1}$, with a maximum value of $79.6 \mu\text{mol NH}_4^+ \text{ L}^{-1}$. Such a high enrichment (30%) was chosen to minimize dilution effects of the ^{15}N source pool over the course of the experiment. At the start and end of the experiment, three replicate water samples were taken to measure NH_4^+ concentration in the water. The same labeled water was used to perform four experiments, before replacing it with freshwater and a new label for the next runs (based on Bal et al. [2013]). Incubations were performed under artificial light conditions. Lamps were mounted above the flume tank throughout the test section to provide 14 h d^{-1} of light (photosynthetic photon flux density of $550 \mu\text{mol m}^{-2} \text{ s}^{-1}$; measured 35 cm above the sediment surface). The stable isotope was added near the paddles that drive the flow in the flume to ensure mixing. Each incubation experiment lasted for 6 h, and two replicate runs were performed for each configuration. At the end of the 6 h, macrophytes were collected from the test positions, rinsed with tap water to remove excess isotope from the plant surface, and folded into aluminum foil. In addition to the samples collected ($n = 30$ for each species), five specimens per species were randomly selected during the experiments from our species stock, to determine the background ^{15}N signal. The plants were dried in the oven for 48 h at 60°C , and individual biomass was weighed. Dried macrophytes were ground to a fine powder using a ball mill (MM 2000, Retsch). A subsample of about 3 mg of powder per plant was sent to the laboratory for mass spectrometry analysis of the isotope ratio. The samples were analyzed for total N content and ^{15}N -atomic percentage (as $[^{15}\text{N}/\text{total N}] \times 100$) with an Elemental

Analyzer (Thermo Electron FlashEA 1112) and subsequent isotope ratio mass spectrometry (Thermo Delta V - IRMS). For recent guidelines on stable isotope notations, see Coplen (2011).

The ^{15}N atomic fraction of the dissolved N source pool in the water column ($x(^{15}\text{N})_{\text{aq,N}}$) was calculated according to Morris et al. (2013):

$$x(^{15}\text{N})_{\text{aq,N}} = \frac{\left([\text{NH}_4^+]_{\text{tracer}} x(^{15}\text{N})_{\text{tracer}}\right) + \left([\text{NH}_4^+]_{\text{water}} x(^{15}\text{N})_{\text{initial}}\right)}{[\text{NH}_4^+]_{\text{tracer}} + [\text{NH}_4^+]_{\text{water}}} \quad (1)$$

where $x(^{15}\text{N})_{\text{tracer}}$ is the atomic fraction of the added tracer (0.98), $[\text{NH}_4^+]_{\text{water}}$ is $20.7 \pm 3.1 \mu\text{mol NH}_4^+ \text{ L}^{-1}$ (mean \pm SE), and $x(^{15}\text{N})_{\text{initial}}$ is the atomic fraction of the initial water column (assumed to reflect ^{15}N of atmospheric N, 3.7×10^{-3}). To provide an estimate of the change in $^{15}\text{NH}_4^+$ ($\mu\text{mol NH}_4^+ \text{ L}^{-1}$) concentrations between runs (i.e., $[\text{NH}_4^+]_{\text{tracer}}$), mean $^{15}\text{NH}_4^+$ uptake rates ($\mu\text{mol g}^{-1}$ [dry mass {DM}] h^{-1}) for each species were multiplied by their total estimated biomass (g [DM] m^{-2}) and by the incubation time (6 h). Given the large volume of the flume water, the estimated $^{15}\text{NH}_4^+$ tracer concentrations remained high, between 8.0 and 8.8 $\mu\text{mol NH}_4^+ \text{ L}^{-1}$, corresponding to an increase in total water column $[\text{NH}_4^+]$ of between 27.5% and 29.7%.

To calculate the NH_4^+ uptake rate (V in $\mu\text{mol g}^{-1}$ [DM] h^{-1}) of each sample, we followed the equation in Morris et al. (2013):

$$V = [\text{N}]_{\text{DM_sample}} \cdot \frac{\left(x^E(^{15}\text{N})_{\text{DM_sample}}\right)}{\left(x(^{15}\text{N})_{\text{aq,N}} \cdot \Delta t\right)} \quad (2)$$

where $x^E(^{15}\text{N})_{\text{DM_sample}}$ is the ^{15}N excess atom fraction, calculated as the difference between the atomic fraction measured in the biomass of the sample after incubation ($x(^{15}\text{N})_{\text{DM_sample}}$) and the background ^{15}N abundance $x(^{15}\text{N})_{\text{DM_nat.ab}}$ measured on five background specimens for each species ($[3.70 \pm 0.008] \times 10^{-3}$ for *Callitriche* and $[3.69 \pm 0.018] \times 10^{-3}$ for *Groenlandia*); Δt (h) is the incubation time (6 h) and $[\text{N}]_{\text{DM_sample}}$ is the N content of the dry biomass ($\mu\text{mol g}^{-1}$ [DM]) of each sample.

Hydrodynamic measurements

To test the relationship between hydrodynamic parameters and nutrient uptake, vertical profiles of velocity were measured with a 3D acoustic Doppler velocimeter (ADV, Nortek) over 30 s at 10 Hz. Within each profile, velocity was measured at seven vertical locations at 2, 5, 10, 12, 15, 17, and 27 cm above the channel bed. The profiles were measured in the same streamwise and lateral locations as the plant samples collected for nutrient uptake estimation, that is, at 10%, 50%,

and 90% of the length of each patch in the streamwise (x) direction and at 0.15 and 0.25 m of the patch width in the spanwise (y) direction (Fig. 2). To minimize interference by vegetation structures within the sampling volume of the ADV probe, the probe started at the lowest measuring point for each vertical profile within the vegetation. This prevented the canopy from being compressed as the probe moved toward the bed. To ensure that measurements were based on reliable data points, spikes and low-quality data points (i.e., correlation below the standard quality threshold of 70%) were removed during postprocessing. The height of the vegetation canopy in each location was measured with a ruler in centimeter. The canopy height (h) was 0.17 ± 0.08 m for *Callitriche* and 0.07 ± 0.01 m for *Groenlandia* (Table 1). Freshwater macrophytes are flexible, mesh-like structures (Sand-Jensen 2005), often with highly branched stems that get entangled in each other. Their flexibility and complex morphology make it very challenging to measure individual plant parameters like shoot height, frontal area, shoot density, or average distance between shoots. Thus, the frontal area per water volume (a , m^{-1}) and frontal area per bed area (ah , dimensionless) for the two species were calculated from water depth (H) and canopy length (l), width (y), and height (h) measurements (Table 1) through the following equations:

$$a = \frac{hy}{Hy l} = \frac{h}{H l} \quad (3)$$

$$ah = \frac{hy}{yl} = \frac{h}{l} \quad (4)$$

As the frontal area of flexible submerged macrophytes is highly variable (i.e., their shape and canopy height change with flow velocity; Sand-Jensen 2005), the values are indicative for the incoming flow velocity of 0.24 m s^{-1} used in the experiments.

The instantaneous velocity ($u(t)$, $v(t)$, $w(t)$) measured in the streamwise, lateral, and vertical directions, respectively, were separated into time-averages (\bar{U} , \bar{V} , \bar{W}) and instantaneous turbulent fluctuations ($u'(t)$, $v'(t)$, $w'(t)$), for example, as $u'(t) = u(t) - \bar{U}$, and similarly for v and w . The vertical average of the time-averaged velocity in the streamwise direction was used to calculate the depth-averaged velocity ($\langle \bar{U} \rangle$, m s^{-1}) at each profile position. The Total Kinetic Energy (Total KE) per unit mass is defined from the instantaneous velocities (u , v , w), defined as:

$$\text{Total KE} = \frac{1}{2} \left(\overline{u^2} + \overline{v^2} + \overline{w^2} \right) = \text{Turbulent KE} + \text{Mean KE} \quad (5)$$

which can be partitioned into turbulent kinetic energy (Turbulent KE) and mean kinetic energy (Mean KE), defined as (e.g., Kundu et al. 2004):

$$\text{Turbulent KE} = \frac{1}{2} \left(\overline{u'^2} + \overline{v'^2} + \overline{w'^2} \right) \quad (6)$$

$$\text{Mean KE} = \frac{1}{2} (\overline{U}^2 + \overline{V}^2 + \overline{W}^2) \quad (7)$$

The Total KE ($\text{m}^2 \text{s}^{-2}$) provides a better metric for the instantaneous velocity, because it reflects both the time-mean and turbulent fluctuations, and as such it is more relevant to boundary layer dynamics, especially in cases with low time-mean velocity but high Turbulent KE. Specifically, previous studies have suggested that strong instantaneous velocity and/or plant motion can periodically strip away the diffusive sublayer, which, if frequent enough, will enhance flux to the plant surface (Koch 1994; Stevens and Hurd 1997; Huang et al. 2011).

Reynolds shear stress (τ_{xz} , Pa) at the top of the canopy at each location was calculated as:

$$\tau_{xz} = -\rho \overline{u'w'} \quad (8)$$

in which $\rho = 1000 \text{ kg m}^{-3}$ is the density of the flume water.

Volumetric flow rate of water through the patches (Q_c , $\text{m}^3 \text{s}^{-1}$) was calculated as:

$$Q_c = \sum_0^h Q_i \text{ and } Q_i = \gamma(h_i - h_{i-1}) \bar{u}_{h_i} \quad (9)$$

in which h is the canopy height, Q_i the volumetric flow rate of water through the layer ($h_i - h_{i-1}$), γ is the patch width (0.3 m), and \bar{u}_{h_i} the double-averaged u component (i.e., averaged in time and spatially averaged in the two lateral positions) of the velocity at depth h_i .

Measuring channel-scale patterns of ammonium uptake

To investigate how the relationship between hydrodynamic parameters and ammonium uptake develops at the scale of a whole channel, we tested the correlation between the total in-patch NH_4^+ uptake rates and in-patch average hydrodynamic parameters (mean velocity, Turbulent KE, and Total KE). This allowed us to test whether spatial patch configurations that generated higher mean flow velocity, Total KE or Turbulent KE levels within the canopies promoted higher uptake at the channel scale. The total in-patch NH_4^+ uptake rate for each configuration was calculated as the sum of the uptake rates estimated in all sampling points ($n = 6$ per species; Fig. 2). This total uptake was used as an estimate of channel-scale uptake but is not necessarily a measure of total ammonium uptake rates per biomass or aerial cover.

Statistical analyses

The flume incubation experiments yielded $n = 30$ samples per experimental run (i.e., from 3 x -positions \times 2 y -positions \times 5 shoots per position) for each species, and two replicate runs were performed for each configuration. As we were interested in differences in uptake rates among positions within patches,

the average uptake rates of the five shoots per each position were used in subsequent analyses. Friedman's rank-sum test was used to test for the presence of trends in NH_4^+ uptake rates from the upstream to downstream positions along the patches in all replicate runs. The tests were run separately for each species, both for the centerline and for the edge measurement points. To account for the fact that within-patch measurements were not independent from each other, statistical differences in NH_4^+ uptake rates for each species under four flume spatial configurations were tested using nested ANOVA (with replicate run as a nested factor within the configuration treatment). As Friedman's rank-sum tests showed no significant trend in ammonium uptake neither along the centerline nor along the edge positions within patches, measurement position was considered a random effect in the model. The data were log-transformed to meet the ANOVA test assumptions of normality and homogeneity of variance. Pearson's correlation coefficient was used to test for significant correlation between NH_4^+ uptake rates ($\mu\text{mol g}^{-1} [\text{DM}] \text{ h}^{-1}$) and hydrodynamic parameters (depth-averaged velocity $\langle \bar{U} \rangle$ [m s^{-1}]; Reynolds shear stress τ_{xz} [Pa]; Turbulent KE [$\text{m}^2 \text{s}^{-2}$]; Total KE [$\text{m}^2 \text{s}^{-2}$]; and volumetric flow rate, Q_c [$\text{m}^3 \text{s}^{-1}$]) and between channel total NH_4^+ uptake rates and average hydrodynamic parameters within both species patches (mean velocity, Turbulent KE, and Total KE). P values of less than or equal to 0.05 were considered to be significant. All statistical analyses were performed in R 3.1.2 (R Core Team 2015).

Results

Relationship between canopy hydrodynamic parameters and nutrient uptake

We found that the two macrophyte species affected each other's ammonium uptake rates by altering mean flow velocity ($\langle \bar{U} \rangle$) and turbulence (Turbulent KE). Ammonium uptake rates depended on either mean flow velocity (*Callitriche*) or turbulence (*Groenlandia*), but Total KE was the single best descriptor of uptake rates for both species (Fig. 3; Table 2). Specifically, NH_4^+ uptake rates for the sparse *Groenlandia* were significantly correlated with Turbulent KE ($r = 0.68$, $p < 0.001$) but not with mean flow velocity ($r = -0.20$, $p = 0.35$) (Fig. 3; Table 2). The opposite was true for the dense *Callitriche*: uptake rates were significantly correlated with mean flow velocity ($r = 0.42$, $p = 0.04$) but not with Turbulent KE ($r = 0.34$, $p = 0.1$) (Fig. 3; Table 2). However, Total KE, which is more representative of the instantaneous velocity, described uptake for both species ($r = 0.79$, $p < 0.001$ for *Groenlandia*; $r = 0.45$, $p = 0.03$ for *Callitriche*; and $r = 0.54$, $p < 0.001$ for both species together) (Fig. 3A; Table 2). No significant relationship was found between ammonium uptake rates and either Reynolds shear stress or Q_c (Table 2).

Effects of patch spatial configurations on nutrient uptake

When located upstream, the dense *Callitriche* patch increased turbulence and thereby enhanced the uptake of

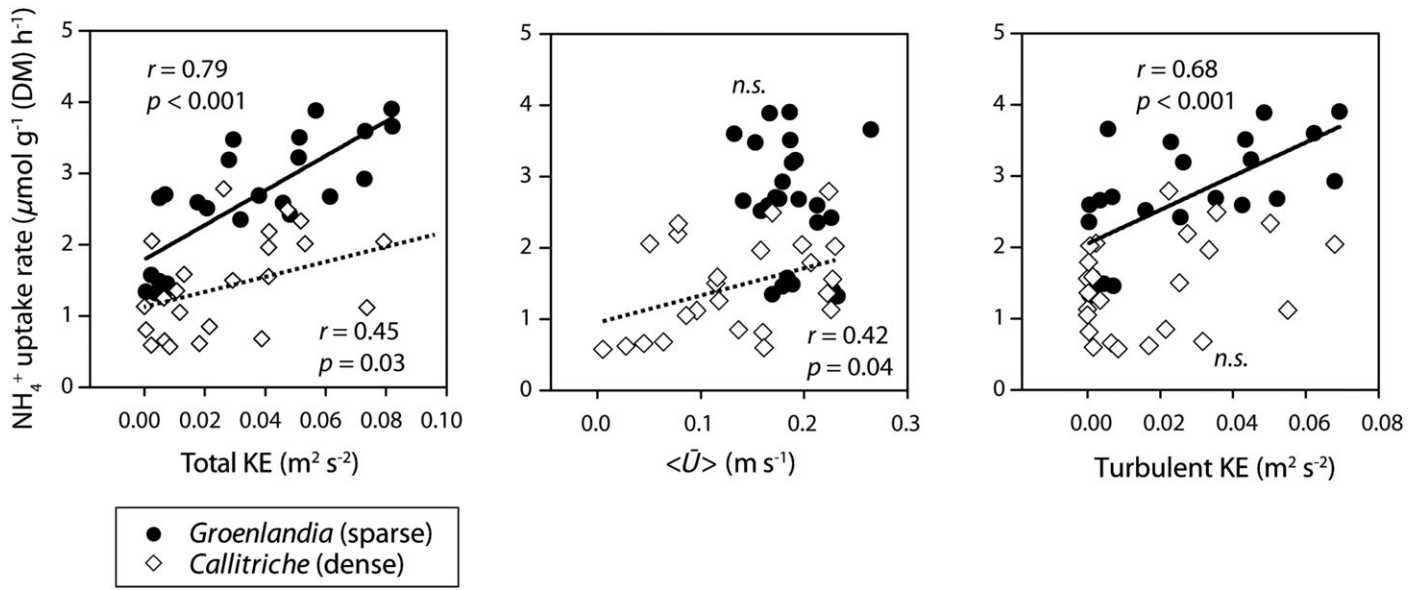


Fig. 3. Scatter plots of NH_4^+ uptake rates ($\mu\text{mol g}^{-1} [\text{DM}] \text{h}^{-1}$) against Total KE ($\text{m}^2 \text{s}^{-2}$), depth-averaged velocity $\langle \bar{U} \rangle$ (m s^{-1}) and turbulent KE ($\text{m}^2 \text{s}^{-2}$) for the sparse *Groenlandia* (black circles) and the dense *Callitriche* (white diamonds). Black lines are linear regression lines for the *Groenlandia* (solid line) and *Callitriche* (dotted line) data separately and represent significant relationships ($p \leq 0.05$).

Table 2. Pearson’s correlation coefficients between NH_4^+ uptake rates ($\mu\text{mol g}^{-1} [\text{DM}] \text{h}^{-1}$) and canopy height (cm) or hydrodynamic parameters (depth-averaged velocity $\langle \bar{U} \rangle$ [m s^{-1}]; Reynolds shear stress τ_{xz} [Pa]; turbulent KE [$\text{m}^2 \text{s}^{-2}$]; Total KE [$\text{m}^2 \text{s}^{-2}$]; and canopy water flow Q_c [$\text{m}^3 \text{s}^{-1}$]) for *Groenlandia*, *Callitriche*, and both species considered together. Correlation coefficients in bold are significant at $p \leq 0.05$.

| | <i>Groenlandia</i> (n = 24) | <i>Callitriche</i> (n = 24) | All (n = 48) |
|---------------------------|--------------------------------|--------------------------------|-----------------|
| Height | 0.17 | -0.18 | -0.30 |
| $\langle \bar{U} \rangle$ | -0.20 | 0.42 | 0.40 |
| τ_{xz} | 0.01 | -0.18 | 0.03 |
| Turbulent KE | 0.68 | 0.34 | 0.53 |
| Total KE | 0.79 | 0.45 | 0.54 |
| Q_c | -0.07 | 0.19 | -0.09 |

resources by the sparse *Groenlandia* patch located downstream. The ammonium uptake rates were influenced by both macrophyte species and spatial patch configuration (order and alignment). Importantly, the D-S configurations led to higher uptake rates for both species. The NH_4^+ uptake rates for the sparse *Groenlandia* were $2.63 \pm 1.33 \mu\text{mol g}^{-1} [\text{DM}] \text{h}^{-1}$, almost double than for the dense *Callitriche* ($1.44 \pm 0.78 \mu\text{mol g}^{-1} [\text{DM}] \text{h}^{-1}$). Testing for the presence of patterns in NH_4^+ uptake rates from upstream to downstream within the patches showed no significant trend in uptake rates neither along the patch centerline (Friedman $\chi^2_2 = 3$, $p = 0.22$ for *Callitriche*; Friedman $\chi^2_2 = 1$, $p = 0.60$ for *Groenlandia*) nor along the patch edge (Friedman $\chi^2_2 = 0.25$, $p = 0.88$ for *Callitriche*; Friedman

$\chi^2_2 = 3$, $p = 0.22$ for *Groenlandia*). This indicates that there was no significant pattern in stable isotope concentration from upstream to downstream within patches.

The upstream–downstream order and spatial patch alignment of the species significantly affected uptake rates for both the sparse *Groenlandia* (nested ANOVA, $F_{3,4} = 6.87$, $p = 0.04$) and the dense *Callitriche* (nested ANOVA, $F_{3,4} = 12.57$, $p = 0.017$; Fig. 4). We generally found that when the denser species (*Callitriche*) was located upstream of the sparser one (*Groenlandia*), ammonium uptake rates for both species increased significantly, compared to patch configurations in the S-D order (Fig. 4). This significant increase in uptake rates was related to the hydrodynamic effects of different configurations, and particularly the traits of *Callitriche* (i.e., density and canopy height, which blocks a larger fraction of flow depth). When the dense patch of *Callitriche* was upstream, it generated higher Turbulent KE that influenced the downstream patch of *Groenlandia* (Fig. 2), enhancing its uptake rates (Fig. 3). Also, when the dense *Callitriche* was upstream, its leading edge was exposed to higher mean velocity compared to when it was trailing behind the sparse patch (Fig. 2), thereby increasing its uptake rates (Fig. 3). Specifically, for the dense *Callitriche*, uptake rates within the S-D order were higher in the staggered than in the aligned configuration (Tukey’s HSD, $z = -2.66$, $p < 0.05$). In the D-S configurations, no significant difference in uptake rates was found between the staggered or aligned arrangement (Tukey’s HSD, $z = -0.50$, $p > 0.05$). However, uptake rates were significantly higher in the D-S staggered configuration than in both the S-D configurations (Tukey’s HSD, $z = -2.83$, $p < 0.05$). For the sparse *Groenlandia*, uptake rates within the S-D aligned and staggered

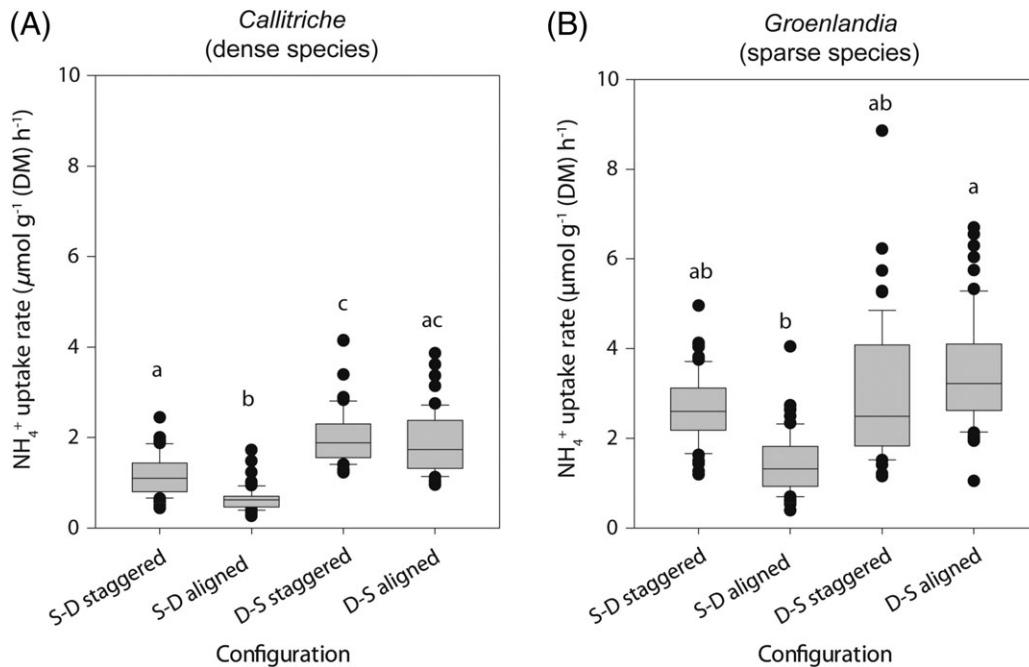


Fig. 4. Boxplots of the distribution of NH_4^+ uptake rates ($\mu\text{mol g}^{-1} [\text{DM}] \text{h}^{-1}$) within patches of the dense *Callitriche* (a) and the sparse *Groenlandia* (b) in each spatial configuration (S indicating sparse vegetation, D indicating dense vegetation; see Fig. 2). Letters denote significant differences (Tukey's HSD, $p < 0.05$).

configuration were not significantly different from each other (Tukey's HSD, $z = -1.92$, $p < 0.05$). In the D-S configurations, no significant difference in uptake rates was found between the staggered or aligned arrangement (Tukey's HSD, $z = 0.51$, $p > 0.05$). Uptake rates in the D-S aligned configuration were significantly higher than in the S-D aligned configuration (Tukey's HSD, $z = -2.69$, $p < 0.05$), but were not significantly different from the S-D staggered case (Tukey's HSD, $z = -0.77$, $p > 0.05$).

We found that the vegetation distributions that generated higher Total KE levels within the patches promoted higher total uptake at the channel scale (Fig. 5). Testing for the hydrodynamic parameter–uptake relationships at the channel scale revealed a significant positive relationship between the in-patch Total KE (average of both patches in each configuration) and the channel total ammonium uptake ($r = 0.98$, $p = 0.01$; Fig. 5). Channel total ammonium uptake was also significantly related to in-patch Turbulent KE ($r = 0.97$, $p = 0.03$) but not to mean flow velocity ($r = 0.93$, $p = 0.07$).

Discussion

The interaction between vegetation and hydrodynamics regulates important ecological processes such as nutrient delivery and uptake by aquatic plants, which are crucial for community primary productivity (Thomas et al. 2000; Cornelisen and Thomas 2006; Morris et al. 2008). We found that, by generating turbulence, dense macrophyte patches facilitate resource uptake by neighboring sparse patches.

Flume measurements showed that the dense *Callitriche* had a strong hydrodynamic effect, creating high-turbulence regions in its wake that facilitated nutrient uptake by the sparse *Groenlandia*, which had a weaker hydrodynamic effect. While the sparse vegetation benefited from the high turbulence generated in the wake of a dense patch, the dense vegetation benefited from being located at a leading edge, where it was

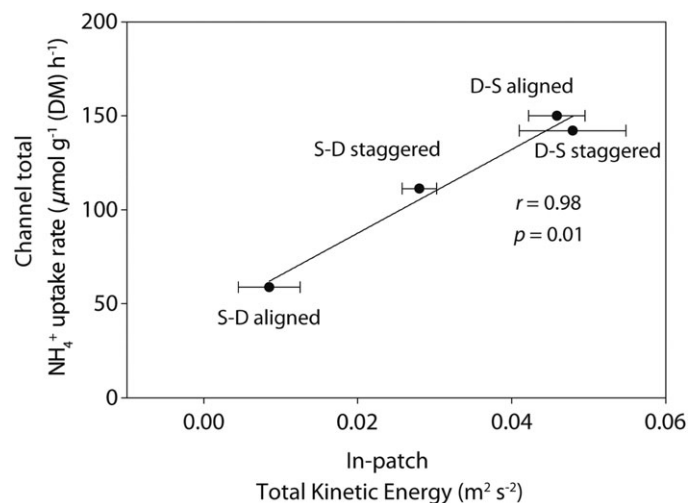


Fig. 5. Scatter plots of channel total NH_4^+ uptake rates ($\mu\text{mol g}^{-1} [\text{DM}] \text{h}^{-1}$) in each spatial configuration against Total KE ($\text{m}^2 \text{s}^{-2}$) averaged within patches of *Callitriche* and *Groenlandia* in each spatial configuration (S indicating sparse vegetation, D indicating dense vegetation; see Fig. 2). Error bars represent standard error of the mean.

exposed to higher mean velocity, compared to when it was located downstream of another patch (Figs. 2, 6). We identified Total KE as the best descriptor of the nutrient removal capacity of streams, especially in heterogeneous multispecies communities. Overall, spatial configurations that lead to higher Total KE within the patches were the ones that led to higher total ammonium uptake. Hence, our results highlight the importance of turbulence as a medium of interaction between different species. Moreover, this study suggests that accounting for interactions between heterogeneous, multispecific patchy vegetation is crucial to understand aquatic ecosystem functions such as nitrogen retention.

Implications of resource uptake in monospecific and multispecific communities

Previous studies of macrophytes generally found that nutrient uptake rates increased with mean flow velocity (Cornelisen and Thomas 2006; Bal et al. 2013). Morris et al. (2008) found that Turbulent KE was associated with spatial variation in uptake, and volumetric flow rate explained differences in uptake between contrasting species. Yet, in our study, neither of these traditional hydrodynamic parameters could accurately describe uptake rates for both species. However, direct comparison with these previous studies is limited to some extent by differences in treatments. While previous experiments tested the effect of changing bulk flow velocity

on uptake rates, we tested a single bulk flow velocity that represented the average flow conditions in the study sites where *Callitriche* and *Groenlandia* coexist. We thus focused on within-patch flow variability and how the interaction between the two species was determined by their spatial arrangement and flow modification. Using a single bulk flow condition resulted in a relatively narrow range of velocities experienced by the sparse *Groenlandia* (0.13–0.27 m s⁻¹), whereas the flow alteration ability of the dense *Callitriche* led to a higher flow variability (0.002–0.24 m s⁻¹). This factor may partly explain the lack of significant correlation between flow velocity and uptake rates for *Groenlandia*. Further research is needed to test how changes in mean flow conditions affect the interaction between the two species.

We identified Total KE as the parameter that explained most of the variability in uptake rates for both species. To our knowledge, this parameter has not been related before to nutrient uptake rates by aquatic vegetation. Previous studies have suggested that Turbulent KE may influence nutrient uptake (Anderson and Charters 1982; Koch 1994), and the total energy parameter captures this influence. Specifically, when Turbulent KE is weak, flux is controlled by the time-mean diffusive sublayer thickness, which is a function of the time-mean velocity (e.g., Hansen et al. 2011; Rominger and Nepf 2014; Lei and Nepf 2016). However, when the Turbulent KE is high, periodic disturbances of the diffusive sublayer by

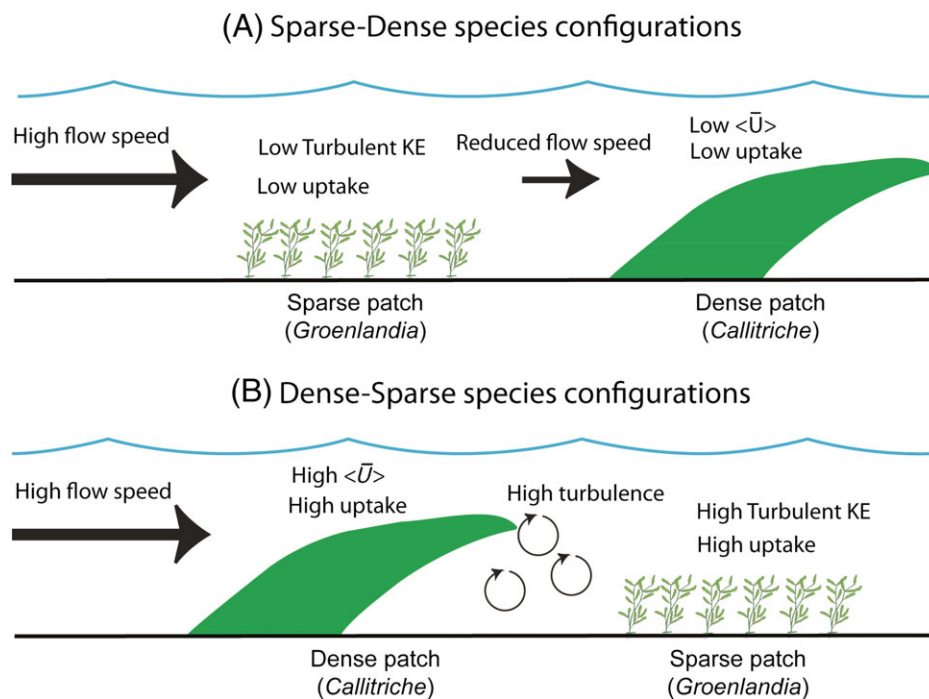


Fig. 6. Schematized drawing of the effects of multispecific spatial patchiness on hydrodynamics and nutrient uptake rates. In S-D configurations (a), the sparse vegetation is exposed to high mean flow but low turbulence, and does not benefit from being located at the leading edge. Similarly, the dense vegetation is exposed to low mean flow speed due to sheltering by the patch upstream, and hence has lower uptake rates. Instead, in D-S configurations (b), uptake rates of both species are higher: The dense vegetation benefits from being at the leading edge and exposed to high mean flow speed (which increases uptake rates); at the same time, the sparse vegetation benefits from the high turbulence created in the wake of the dense patch.

the turbulence can create instantaneously higher concentration gradients at the surface and, thus, higher flux (e.g., Stevens and Hurd 1997; Huang et al. 2011; Rominger and Nepf 2014). By reflecting the magnitude of both the time-mean velocity and Turbulent KE, the Total KE captures both regimes of flux. The Total KE is particularly suitable in heterogeneous systems where upstream Turbulent KE generation (e.g., by larger, denser patches) can influence flux downstream, that is, the Turbulent KE is not locally generated and thus uncorrelated with the local time-mean velocity. In the dense *Callitriche* patches, the canopy is often too dense for turbulence to form within the patch or to penetrate from the free stream. Under these low Turbulent KE conditions, the flux is correlated by the local time-mean velocity, which sets the scale of the diffusive sublayer. For the sparse *Groenlandia*, time-mean flow velocity is relatively constant in the canopy and we found no correlation between within-patch flow variations and uptake rates. However, the within-patch Turbulent KE is elevated both by local stem generation and the penetration of turbulence generated upstream. Under these high Turbulent KE conditions, the uptake rates have a high correlation with the Turbulent KE intensity. In landscapes made up of patches of different species, regions with flux controlled by $\langle \bar{U} \rangle$ and regions controlled by Turbulent KE are heterogeneously distributed, so that neither $\langle \bar{U} \rangle$ nor Turbulent KE can capture the channel-scale nutrient uptake. Because it can describe both regions of low Turbulent KE (uptake controlled by mean velocity) and high Turbulent KE (uptake controlled by Turbulent KE intensity), we propose Total KE as a useful parameter to describe nutrient uptake capacity in heterogeneous landscapes, which could be used to estimate ecosystem services of nutrient retention by vegetation.

In contrast to the findings of Morris et al. (2008) and Bal et al. (2013), we did not find a significant relationship between ammonium uptake rates and volumetric flow rate, likely because the two species have different flexibility and density traits that affect patch compression (Table 1). The canopies of the two species, and the relative importance of flow velocity and turbulence within them, are consistent with the sparse and dense canopy regimes described in Nepf (2012). As expected for a dense canopy condition ($ah > 0.1$), canopy-scale turbulence in *Callitriche* is generated at the top of the canopy and can be transported downstream, while stem-scale turbulence is much smaller. Instead, *Groenlandia* is representative of a sparse canopy condition ($ah < 0.1$), where stem-scale turbulence is generated within the canopy, but the velocity profile remains logarithmic.

Our results reveal the important role of patch spatial configuration and the resulting heterogeneity in influencing species interactions and the nutrient uptake capacity of the landscape. The generation of turbulence by a *Callitriche* patch led to a 59% nutrient uptake enhancement effect on *Groenlandia*, increasing it from an ammonium uptake rate of $2.03 \pm 0.85 \mu\text{mol g}^{-1} [\text{DM}] \text{ h}^{-1}$ in the S-D configurations

(where *Groenlandia* was not exposed to turbulence generation by *Callitriche*), to $3.23 \pm 0.37 \mu\text{mol g}^{-1} [\text{DM}] \text{ h}^{-1}$ in the D-S configurations (where it was exposed to turbulence generation by *Callitriche*). These findings are in line with a field study showing that spatial heterogeneity, created by the interaction of canopy morphology, sediment topography, and hydrodynamics, controlled nutrient transport and uptake rates in a patchy seagrass landscape (Morris et al. 2013). While we found clear effects of the upstream–downstream patch arrangement on ammonium uptake rates, we only observed a significant effect of patch arrangement (staggered vs. aligned) in the S-D configurations. Vegetation patches in the flume experiment did not span the whole width of the channel, leading to water flow deflection and acceleration around the lateral edges of patches. This flow acceleration effect around the patches is in general agreement with experimental evidence in field and laboratory studies (Vandenbruwaene et al. 2011; Schoelynck et al. 2012; Bouma et al. 2013), suggesting that the conclusions of this work could be generally applied to field conditions. In addition to the role of spatial configuration, it is likely that the distance between the patches governs the intensity of the interaction between them. The stronger interactions between patches likely occur when the distance between them is less than the wake length of the upstream patch (Folkard 2005). It might be expected that the wake length is in turn related to patch density, because density determines at what distances the patch effects will dissipate (Zong and Nepf 2012). Further studies should be undertaken to investigate the detailed hydrodynamic consequences of different spatial patch configurations, testing for the effects of a wider range of distances and its interactive effect with patch density.

Turbulence-mediated species interactions: Implications for species distributions and nutrient load reduction

The study of turbulence-mediated interactions between macrophyte species suggests a possible mechanism behind the co-occurrence of *Groenlandia* patches around *Callitriche* in the field. Recently, it has been shown that *Groenlandia* shoots grow better around *Callitriche* patches than on bare, unvegetated sediment (Cornacchia et al. 2018). The wake of the *Callitriche* patches is both a high-turbulence and low-velocity region (Sand-Jensen 1998). Thus, a combination of enhanced resource uptake by turbulence and reduced biomass losses by flow velocity might be the conditions behind the improved growth rates of *Groenlandia* plants around *Callitriche* patches. As the sparse *Groenlandia* tends to surround the dense *Callitriche* patches in regularly spaced aggregations every 8 m (Cornacchia et al. 2018), the interaction between the two species might enhance the overall nutrient removal capacity of the river. The facilitative effect of *Callitriche* on *Groenlandia* could switch to competition, as the high biomass *Callitriche* might have a competitive advantage by reducing resource availability for the sparser species (*Groenlandia*). Conversely,

competition could be lessened through root uptake from the nutrient pool in the sediment. The balance between facilitation and competition can be clarified by considering additional variables such as root uptake and nutrient availability in the water column and in sediment. Moreover, care must be taken when upscaling the relationship between hydrodynamics and resource uptake at the channel scale. In our incubations, we focused only on uptake rates of a single nutrient (ammonium), which is energetically less costly, but some species might invest in nitrate uptake. This is an interesting aspect that should be explored in future studies of channel-scale nitrogen uptake by vegetation. As a future perspective, we might be able to use the knowledge on these types of species interactions as tools to enhance restoration success of degraded (eutrophic) sites.

References

- Adhitya, A. and others 2014. Comparison of the influence of patch-scale and meadow-scale characteristics on flow within seagrass meadows: A flume study. *Mar. Ecol. Prog. Ser.* **516**: 49–59. doi:10.3354/meps10873
- Anderson, S. M., and A. Charters. 1982. A fluid dynamics study of seawater flow through *Gelidium nudifrons*. *Limnol. Oceanogr.* **27**: 399–412. doi:10.4319/lo.1982.27.3.0399
- Bal, K. D. and others 2013. Influence of hydraulics on the uptake of ammonium by two freshwater plants. *Freshwater Biol.* **58**: 2452–2463. doi:10.1111/fwb.12222
- Bouma, T., M. Friedrichs, B. Van Wesenbeeck, S. Temmerman, G. Graf, and P. Herman. 2009. Density-dependent linkage of scale-dependent feedbacks: A flume study on the intertidal macrophyte *Spartina anglica*. *Oikos* **118**: 260–268. doi:10.1111/j.1600-0706.2008.16892.x
- Bouma, T. and others 2005. Trade-offs related to ecosystem engineering: A case study on stiffness of emerging macrophytes. *Ecology* **86**: 2187–2199. doi:10.1890/04-1588
- Bouma, T. and others 2007. Spatial flow and sedimentation patterns within patches of epibenthic structures: Combining field, flume and modelling experiments. *Cont. Shelf Res.* **27**: 1020–1045. doi:10.1016/j.csr.2005.12.019
- Bouma, T. and others 2013. Organism traits determine the strength of scale-dependent bio-geomorphic feedbacks: A flume study on three intertidal plant species. *Geomorphology* **180**: 57–65. doi:10.1016/j.geomorph.2012.09.005
- Chen, Z., A. Ortiz, L. Zong, and H. Nepf. 2012. The wake structure behind a porous obstruction and its implications for deposition near a finite patch of emergent vegetation. *Water Resour. Res.* **48**: W09517. doi:10.1029/2012WR012224
- Chen, Z., C. Jiang, and H. Nepf. 2013. Flow adjustment at the leading edge of a submerged aquatic canopy. *Water Resour. Res.* **49**: 5537–5551. doi:10.1002/wrcr.20403
- Coplen, T. B. 2011. Guidelines and recommended terms for expression of stable-isotope-ratio and gas-ratio measurement results. *Rapid Commun. Mass Spectrom.* **25**: 2538–2560. doi:10.1002/rcm.5129
- Corenblit, D. and others 2011. Feedbacks between geomorphology and biota controlling earth surface processes and landforms: A review of foundation concepts and current understandings. *Earth-Sci. Rev.* **106**: 307–331. doi:10.1016/j.earscirev.2011.03.002
- Cornacchia, L., J. van de Koppel, D. van der Wal, G. Wharton, S. Puijalon, and T. J. Bouma. 2018. Landscapes of facilitation: How self-organized patchiness of aquatic macrophytes promotes diversity in streams. *Ecology* **99**: 832–847. doi:10.1002/ecy.2177
- Cornelisen, C. D., and F. I. Thomas. 2004. Ammonium and nitrate uptake by leaves of the seagrass *Thalassia testudinum*: Impact of hydrodynamic regime and epiphyte cover on uptake rates. *J. Mar. Syst.* **49**: 177–194. doi:10.1016/j.jmarsys.2003.05.008
- Cornelisen, C. D., and F. I. Thomas. 2006. Water flow enhances ammonium and nitrate uptake in a seagrass community. *Mar. Ecol. Prog. Ser.* **312**: 1–13. doi:10.3354/meps312001
- Cotton, J., G. Wharton, J. Bass, C. Heppell, and R. Wotton. 2006. The effects of seasonal changes to in-stream vegetation cover on patterns of flow and accumulation of sediment. *Geomorphology* **77**: 320–334. doi:10.1016/j.geomorph.2006.01.010
- Dawson, F., and W. Robinson. 1984. Submerged macrophytes and the hydraulic roughness of a lowland chalkstream. *Verhandlung Int. Vereinigung Limnol.* **22**: 1944–1948. doi:10.1080/03680770.1983.11897598
- Dietrich, W. E., and J. T. Perron. 2006. The search for a topographic signature of life. *Nature* **439**: 411–418. doi:10.1038/nature04452
- Folkard, A. M. 2005. Hydrodynamics of model *Posidonia oceanica* patches in shallow water. *Limnol. Oceanogr.* **50**: 1592–1600. doi:10.4319/lo.2005.50.5.1592
- Follett, E. M., and H. M. Nepf. 2012. Sediment patterns near a model patch of reedy emergent vegetation. *Geomorphology* **179**: 141–151. doi:10.1016/j.geomorph.2012.08.006
- Fonseca, M. S., J. C. Zieman, G. W. Thayer, and J. S. Fisher. 1983. The role of current velocity in structuring eelgrass (*Zostera marina* L.) meadows. *Estuar. Coast. Shelf Sci.* **17**: 367–380. doi:10.1016/0272-7714(83)90123-3
- Gambi, M. C., A. R. Nowell, and P. A. Jumars. 1990. Flume observations on flow dynamics in *Zostera marina* (eelgrass) beds. *Mar. Ecol. Prog. Ser.* **61**: 159–169. doi:10.3354/meps061159
- Hansen, A. T., M. Hondzo, and C. L. Hurd. 2011. Photosynthetic oxygen flux by *Macrocystis pyrifera*: A mass transfer model with experimental validation. *Mar. Ecol. Prog. Ser.* **434**: 45–55. doi:10.3354/meps09196
- Haynes, R., and K. M. Goh. 1978. Ammonium and nitrate nutrition of plants. *Biol. Rev.* **53**: 465–510. doi:10.1111/j.1469-185X.1978.tb00862.x

- Huang, I., J. Rominger, and H. Nepf. 2011. The motion of kelp blades and the surface renewal model. *Limnol. Oceanogr.* **56**: 1453–1462. doi:[10.4319/lo.2011.56.4.1453](https://doi.org/10.4319/lo.2011.56.4.1453)
- Järvelä, J. 2005. Effect of submerged flexible vegetation on flow structure and resistance. *J. Hydrol.* **307**: 233–241. doi:[10.1016/j.jhydrol.2004.10.013](https://doi.org/10.1016/j.jhydrol.2004.10.013)
- Jones, C. G., J. H. Lawton, and M. Shachak. 1994. Organisms as ecosystem engineers, p. 130–147. *In* Ecosystem management. Springer. doi:[10.1016/S0272-6386\(12\)80823-7](https://doi.org/10.1016/S0272-6386(12)80823-7)
- Koch, E. 1994. Hydrodynamics, diffusion-boundary layers and photosynthesis of the seagrasses *Thalassia testudinum* and *Cymodocea nodosa*. *Mar. Biol.* **118**: 767–776. doi:[10.1007/BF00347527](https://doi.org/10.1007/BF00347527)
- Kouwen, N., and T. E. Unny. 1973. Flexible roughness in open channels. *J. Hydraul. Div.* **99**: 713–728.
- Kundu, P. K., I. M. Cohen, and H. H. Hu. 2004. Fluid mechanics, 6th ed. Elsevier Press.
- Lei, J., and H. Nepf. 2016. Impact of current speed on mass flux to a model flexible seagrass blade. *J. Geophys. Res. Oceans* **121**: 4763–4776. doi:[10.1002/2016JC011826](https://doi.org/10.1002/2016JC011826)
- Leonard, L. A., and M. E. Luther. 1995. Flow hydrodynamics in tidal marsh canopies. *Limnol. Oceanogr.* **40**: 1474–1484. doi:[10.4319/lo.1995.40.8.1474](https://doi.org/10.4319/lo.1995.40.8.1474)
- Levi, P. S. and others 2015. Macrophyte complexity controls nutrient uptake in lowland streams. *Ecosystems* **18**: 914–931. doi:[10.1007/s10021-015-9872-y](https://doi.org/10.1007/s10021-015-9872-y)
- Madsen, J. D., P. A. Chambers, W. F. James, E. W. Koch, and D. F. Westlake. 2001. The interaction between water movement, sediment dynamics and submersed macrophytes. *Hydrobiologia* **444**: 71–84. doi:[10.1023/A:1017520800568](https://doi.org/10.1023/A:1017520800568)
- Madsen, T. V., and N. Cedergreen. 2002. Sources of nutrients to rooted submerged macrophytes growing in a nutrient-rich stream. *Freshwater Biol.* **47**: 283–291. doi:[10.1046/j.1365-2427.2002.00802.x](https://doi.org/10.1046/j.1365-2427.2002.00802.x)
- Meire, D. W., J. M. Kondziolka, and H. M. Nepf. 2014. Interaction between neighboring vegetation patches: Impact on flow and deposition. *Water Resour. Res.* **50**: 3809–3825. doi:[10.1002/2013WR015070](https://doi.org/10.1002/2013WR015070)
- Morris, E. P., G. Peralta, F. G. Brun, L. Van Duren, T. J. Bouma, and J. L. Perez-Llorens. 2008. Interaction between hydrodynamics and seagrass canopy structure: Spatially explicit effects on ammonium uptake rates. *Limnol. Oceanogr.* **53**: 1531–1539. doi:[10.4319/lo.2008.53.4.1531](https://doi.org/10.4319/lo.2008.53.4.1531)
- Morris, E. P. and others 2013. The role of hydrodynamics in structuring in situ ammonium uptake within a submerged macrophyte community. *Limnol. Oceanogr.: Fluids Environ.* **3**: 210–224. doi:[10.1215/21573689-2397024](https://doi.org/10.1215/21573689-2397024)
- Nepf, H. 1999. Drag, turbulence, and diffusion in flow through emergent vegetation. *Water Resour. Res.* **35**: 479–489. doi:[10.1029/1998WR900069](https://doi.org/10.1029/1998WR900069)
- Nepf, H., and E. Vivoni. 2000. Flow structure in depth-limited, vegetated flow. *J. Geophys. Res. Oceans* **105**: 28547–28557. doi:[10.1029/2000JC900145](https://doi.org/10.1029/2000JC900145)
- Nepf, H. M. 2012. Flow and transport in regions with aquatic vegetation. *Annu. Rev. Fluid Mech.* **44**: 123–142. doi:[10.1146/annurev-fluid-120710-101048](https://doi.org/10.1146/annurev-fluid-120710-101048)
- Peralta, G., L. Van Duren, E. Morris, and T. Bouma. 2008. Consequences of shoot density and stiffness for ecosystem engineering by benthic macrophytes in flow dominated areas: A hydrodynamic flume study. *Mar. Ecol. Prog. Ser.* **368**: 103–115. doi:[10.3354/meps07574](https://doi.org/10.3354/meps07574)
- R Core Team. 2015. R: A language and environment for statistical computing (version 3.1. 2): R foundation for statistical computing. Available from <http://www.R-project.org>. Last accessed on 27 April 2018.
- Rominger, J. T., and H. M. Nepf. 2014. Effects of blade flexural rigidity on drag force and mass transfer rates in model blades. *Limnol. Oceanogr.* **59**: 2028–2041. doi:[10.4319/lo.2014.59.6.2028](https://doi.org/10.4319/lo.2014.59.6.2028)
- Sand-Jensen, K. 1998. Influence of submerged macrophytes on sediment composition and near-bed flow in lowland streams. *Freshwater Biol.* **39**: 663–679. doi:[10.1046/j.1365-2427.1998.00316.x](https://doi.org/10.1046/j.1365-2427.1998.00316.x)
- Sand-Jensen, K. 2005. Aquatic plants are open flexible structures—a reply to Sukhodolov. *Freshwater Biol.* **50**: 196–198. doi:[10.1111/j.1365-2427.2004.01297.x](https://doi.org/10.1111/j.1365-2427.2004.01297.x)
- Sand-Jensen, K., and T. Vindbæk Madsen. 1992. Patch dynamics of the stream macrophyte, *Callitriche cophocarpa*. *Freshwater Biol.* **27**: 277–282. doi:[10.1111/j.1365-2427.1992.tb00539.x](https://doi.org/10.1111/j.1365-2427.1992.tb00539.x)
- Schoelynck, J., T. De Groote, K. Bal, W. Vandenbruwaene, P. Meire, and S. Temmerman. 2012. Self-organised patchiness and scale-dependent bio-geomorphic feedbacks in aquatic river vegetation. *Ecography* **35**: 760–768. doi:[10.1111/j.1600-0587.2011.07177.x](https://doi.org/10.1111/j.1600-0587.2011.07177.x)
- Schulz, M., H.-P. Kozerski, T. Pluntke, and K. Rinke. 2003. The influence of macrophytes on sedimentation and nutrient retention in the lower river spree (Germany). *Water Res.* **37**: 569–578. doi:[10.1016/S0043-1354\(02\)00276-2](https://doi.org/10.1016/S0043-1354(02)00276-2)
- Sheldon, R. B., and C. W. Boylen. 1977. Maximum depth inhabited by aquatic vascular plants. *Am. Midl. Nat.* **97**: 248–254. doi:[10.2307/2424706](https://doi.org/10.2307/2424706)
- Stevens, C. L., and C. L. Hurd. 1997. Boundary-layers around bladed aquatic macrophytes. *Hydrobiologia* **346**: 119–128. doi:[10.1023/A:1002914015683](https://doi.org/10.1023/A:1002914015683)
- Thomas, F. I., C. D. Cornelisen, and J. M. Zande. 2000. Effects of water velocity and canopy morphology on ammonium uptake by seagrass communities. *Ecology* **81**: 2704–2713. doi:[10.1890/0012-9658\(2000\)081\[2704:EOWVAC\]2.0.CO;2](https://doi.org/10.1890/0012-9658(2000)081[2704:EOWVAC]2.0.CO;2)
- Vandenbruwaene, W. and others 2011. Flow interaction with dynamic vegetation patches: Implications for biogeomorphic evolution of a tidal landscape. *J. Geophys. Res. Earth* **116**: F01008. doi:[10.1029/2010JF001788](https://doi.org/10.1029/2010JF001788)
- Weitzman, J. S., R. B. Zeller, F. I. Thomas, and J. R. Koseff. 2015. The attenuation of current-and wave-driven flow within submerged multispecific vegetative canopies. *Limnol. Oceanogr.* **60**: 1855–1874. doi:[10.1002/lno.10121](https://doi.org/10.1002/lno.10121)

- Wharton, G. and others 2006. Macrophytes and suspension-feeding invertebrates modify flows and fine sediments in the Frome and piddle catchments, Dorset (UK). *J. Hydrol.* **330**: 171–184. doi:[10.1016/j.jhydrol.2006.04.034](https://doi.org/10.1016/j.jhydrol.2006.04.034)
- Zong, L., and H. Nepf. 2012. Vortex development behind a finite porous obstruction in a channel. *J. Fluid Mech.* **691**: 368–391. doi:[10.1017/jfm.2011.479](https://doi.org/10.1017/jfm.2011.479)

Acknowledgments

The authors gratefully acknowledge Bert Sinke, Lennart van IJzerloo, Lowie Haazen, and Jeroen van Dalen for their technical assistance in the flume. We thank Peter van Breugel and members of the analytical lab of NIOZ-Yerseke for the stable isotope analyses. We thank Siebren Wezenberg for helping during the experiments. This work was supported by the Research Executive Agency, through the 7th Framework Programme of

the European Union, Support for Training and Career Development of Researchers (Marie Curie - FP7-PEOPLE-2012-ITN), which funded the Initial Training Network (ITN) HYTECH “Hydrodynamic Transport in Ecologically Critical Heterogeneous Interfaces,” N.316546. Data associated with this study is available from 4TU. Centre for Research Data at: [10.4121/uuid:e4678efa-426f-483a-b74a-c6ab4df53354](https://doi.org/10.4121/uuid:e4678efa-426f-483a-b74a-c6ab4df53354).

Conflict of Interest

None declared.

Submitted 03 November 2017

Revised 07 October 2018

Accepted 09 October 2018

Associate editor: Josef Daniel Ackerman